Supplemental Figure 1

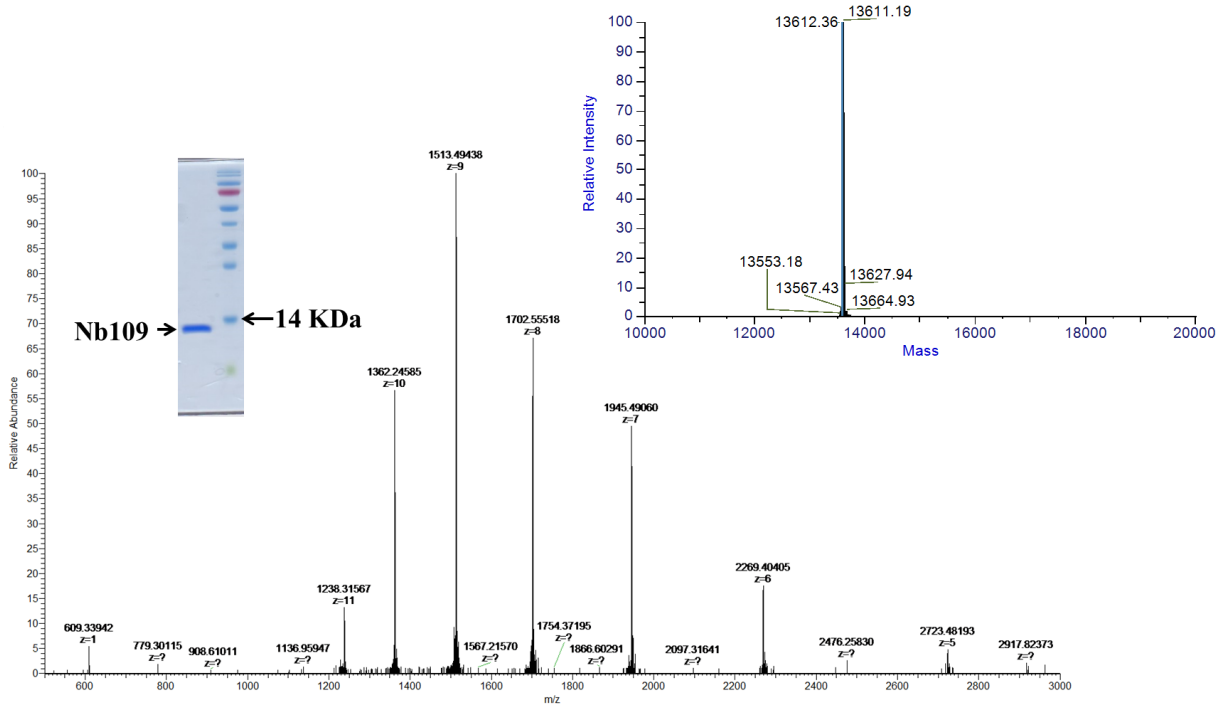

Supplemental Figure 1 The SDS-PAGE and ESI-Q-TOF-MS characterization of Nb109.

Supplemental Figure 2

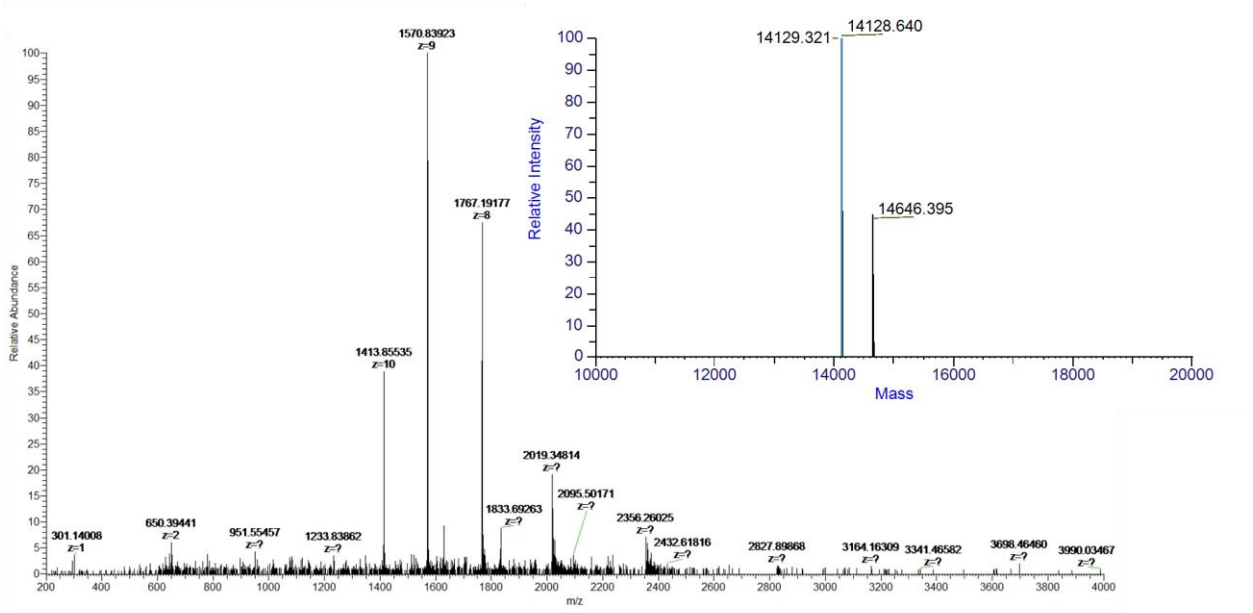

Supplemental Figure 2 The ESI-Q-TOF-MS of NOTA-Nb109.

Supplemental Figure 3

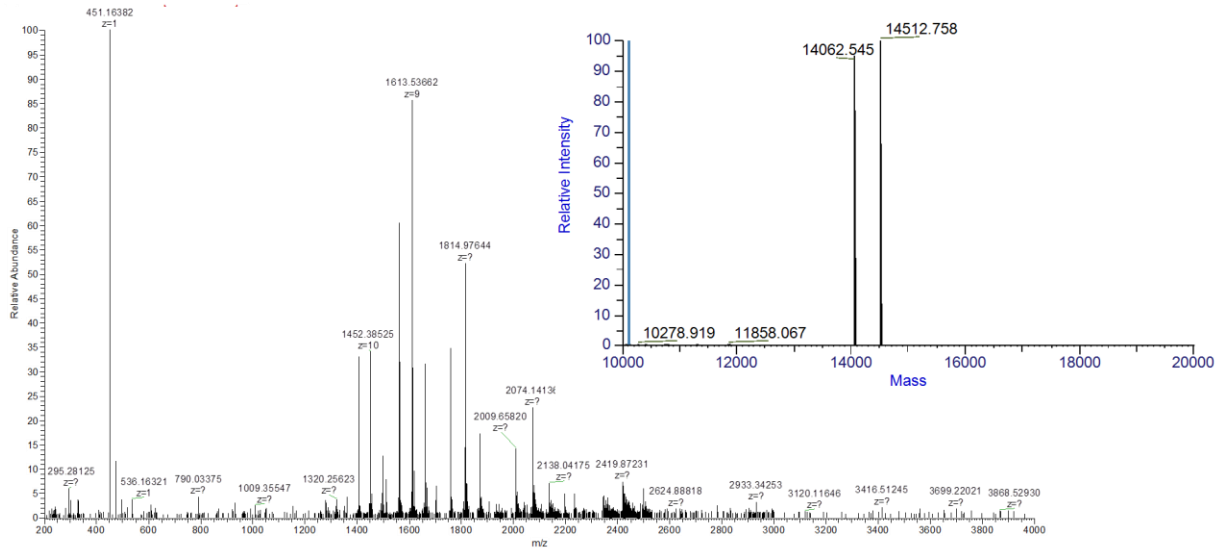

Supplemental Figure 3 The ESI-Q-TOF-MS of ^{69}Ga-NOTA-Nb109.

Supplemental Figure 4

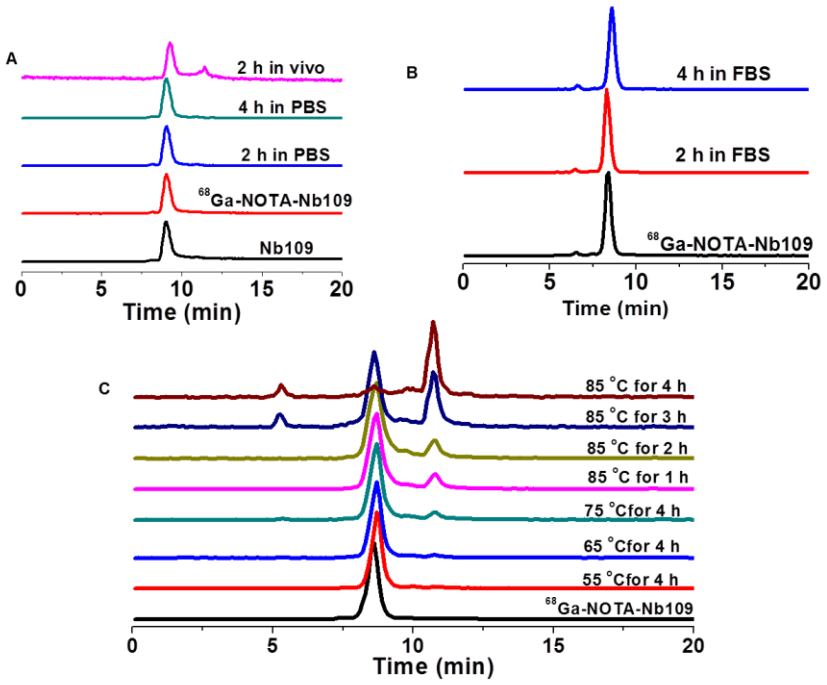

Supplemental Figure 4 In vitro stability of ^{68}Ga-NOTA-Nb109 in (A) PBS (pH 7.4) and urine and (B) fetal bovine serum (FBS) at different time under 37 °C; (C) the thermal stability of ^{68}Ga-NOTA-Nb109 under different temperature. Nb109: UV detector (320 nm), ^{68}Ga-NOTA-Nb109: radioactive detector.

Supplemental Figure 5

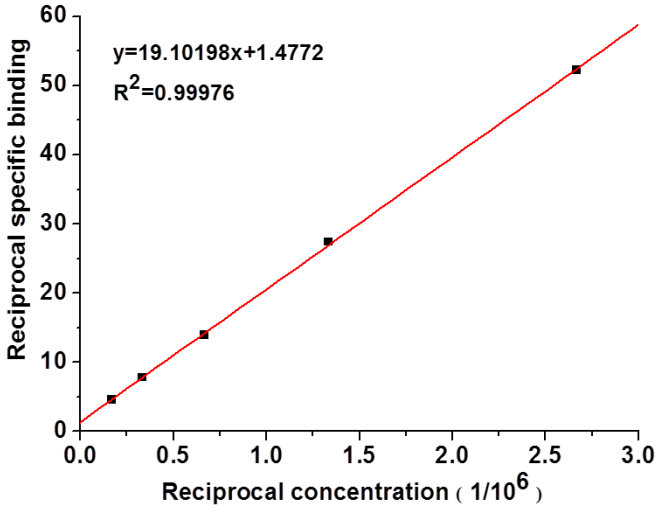

Supplemental Figure 5 The immunoreactivity assay of ^{68}Ga-NOTA-Nb109.

Supplemental Figure 6

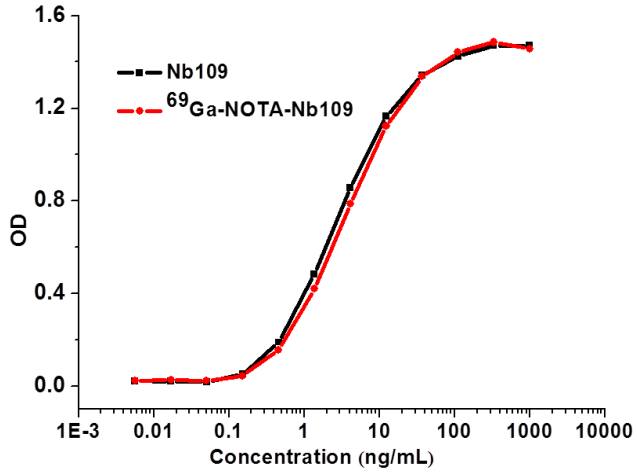

Supplemental Figure 6 The binding curves of Nb109 (black) and ^{68}Ga-NOTA-Nb109 (red) to PD-L1 assessed by ELISA.

Supplemental Figure 7

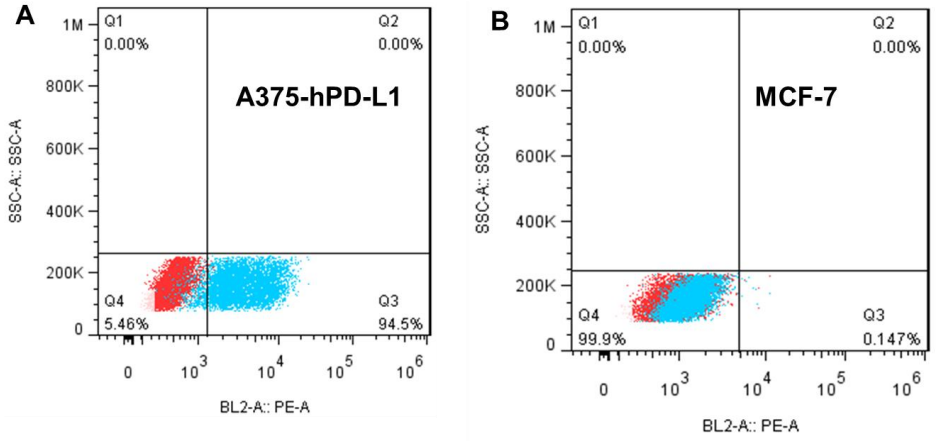

Supplemental Figure 7 The expression of PD-L1 in A375-hPD-L1 (A) and MCF-7 (B) cell lines measured by flow cytometry.

Supplemental Figure 8

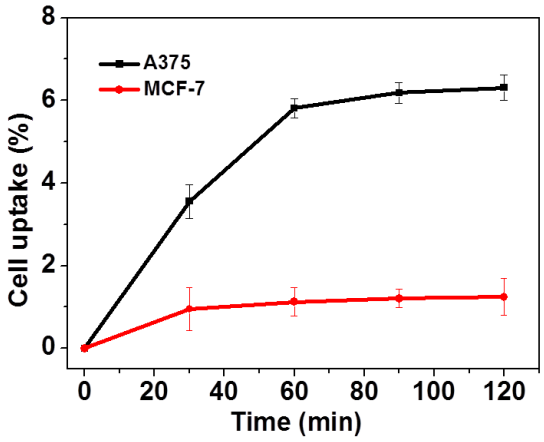

Supplemental Figure 8 The cellular uptake of ^{68}Ga-NOTA-Nb109 in A375-hPD-L1 (black) and MCF-7 (red) cell lines at different time points.

Supplemental Figure 9

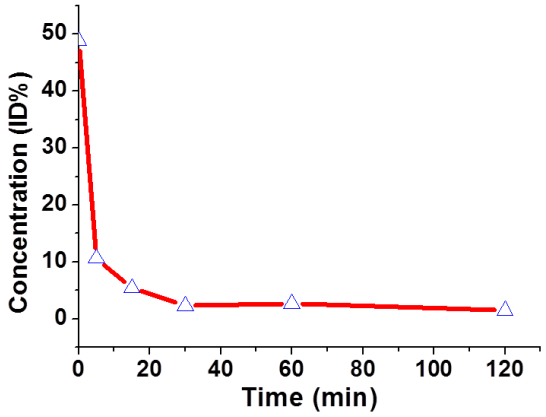

Parameter	Unit	Value
$t_{1/2}$	min	49.79
T_{max}	min	0.10
C_{max}	ID%	48.82
C_0	ID%	50.37
AUC_{0-t}	ID%*min	487.03
AUC_{0-inf}	ID%*min	593.39
MRT_{0-inf}	min	60.53
V_z	(μci)/(ID%)	11.41
CL	(μci)/(ID%)/min	0.15
V_{ss}	(μci)/(ID%)	9.61

Supplemental Figure 9 The pharmacokinetic behavior of ^{68}Ga-NOTA-Nb109.

Supplemental Figure 10

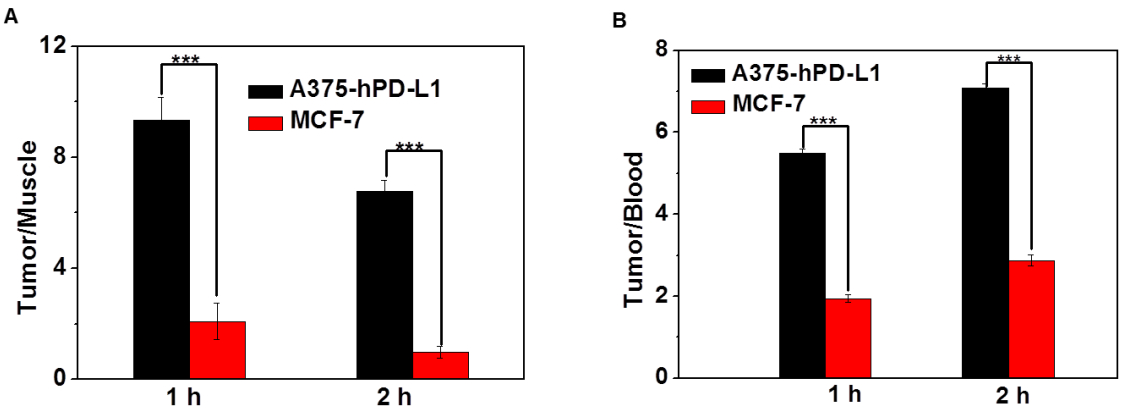

Supplemental Figure 10 The tumor-to-muscle (A) and tumor-to-blood (B) ratios at 1 h and 2 h post injection of ^{68}Ga-NOTA-Nb109 in tumor-bearing models, respectively. ***, $p < 0.001$..